Dual-Band Reflectarray Project Report: Spring 2025

Fatemeh Sadr, Jordan Budhu, and Steven Ellingson
Virginia Tech, Blacksburg, VA, USA

I. Abstract

This report presents the design and analysis of a dual-band reflectarray antenna operating at 1.62125 GHz in the L-band and 11.7 GHz in the X-band.

The objective of this work is to realize a widely separated dual-frequency reflectarray implemented using a novel structure, while enabling independent control of each frequency band. The proposed design introduces strategically placed ground-plane slots to realize one of the operating bands, while not impacting the performance of the other. This approach reduces structural complexity while mitigating mutual blockage and electromagnetic interference between the two bands.

Simulation results demonstrate minimal performance degradation for each band in the presence of the other. Specifically, the introduction of the L-band ground-plane slots does not significantly affect the X-band gain, beam direction, or radiation efficiency. Similarly, the presence of the X-band elements has a negligible impact on the L-band radiation pattern, as the X-band structure behaves as an approximately uniform impedance sheet at L-band frequencies, which is accounted for in the L-band design. As a result, the gain, beam shape, and overall efficiency remain consistent when both bands operate simultaneously.

These results validate the independent operation of the two frequency bands within the proposed architecture and confirm the effectiveness of the proposed design approach. The proposed antenna is therefore a candidate for applications such as radio astronomy, where operating at multiple frequencies is required while mitigating interference from satellite signals [1]–[4]

II. Introduction

Dual-band reflectarray antennas have attracted considerable attention due to their ability to support multi-frequency operation within a single aperture. However, the design of reflectarrays operating at widely separated frequency bands remains a challenging problem.

One of the primary challenges in designing a widely separated dual-band reflectarray arises from the large disparity between the wavelengths of the two operating bands. In this work, the wavelength at the lower-band center frequency is approximately 7.2 times of that of the upper-band center frequency. This ratio leads to a substantial difference in unit-cell dimensions, making the implementation of both bands in a single aperture particularly difficult due to strong mutual coupling effects. Alternatively, multilayer configurations often suffer from severe electromagnetic blockage, as the electrically large L-band elements can perturb the performance at X-band structures when placed above or below them.

The main contribution of this work is to eliminate the need for one of the metallic radiating structures, either on the same layer or across multiple layers. To achieve this, a novel unit-cell architecture is proposed in which ground-plane slots cut into the ground plane of the higher frequency elements are employed as the radiating and phase-controlling elements for the lower frequency elements. This approach removes the requirement for an additional metallic layer, reducing structural complexity, and effectively mitigating mutual blockage between the two bands.

The proposed dual-band reflectarray operates at widely separated frequency ranges, specifically at (11.7 GHz) and (1.6125 GHz). To enable independent operation at both frequencies while maintaining high radiation efficiency, a novel unit cell is designed, as illustrated in Fig. 1. The unit cell consists of two distinct mechanisms for phase control: a metallic structure for X-band operation and a ground-plane slot for L-band operation. This configuration allows each frequency band to be independently controlled with minimal electromagnetic interference between them. The geometrical dimensions of the different parts of the unit cell are summarized in Table I.

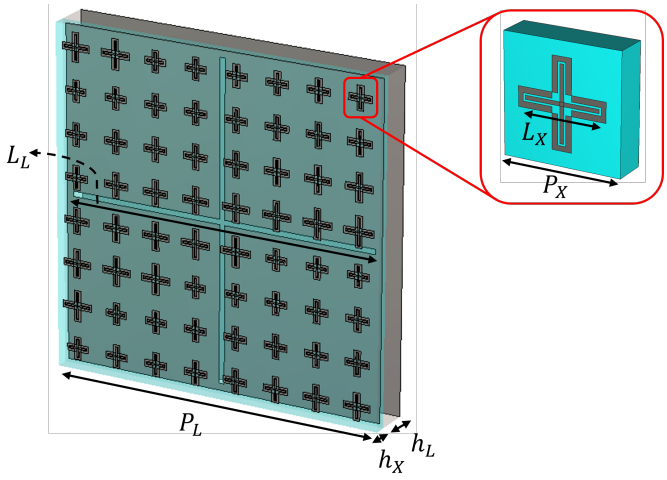

Fig. 1: Perspective view of the dual-band unit cell, showing the detailed geometry of the elements.

As shown in Fig. 1, the proposed unit cell is realized using a multilayer stackup. Starting from the top, the structure consists of an X-band cross-shaped slot layer, followed by a dielectric spacer with a thickness of h_X. The L-band layer contains a crossed-shaped slot etched in the ground plane, which also acts as the effective ground plane for the X-band layer. A second dielectric spacer with a thickness of h_L is introduced beneath the L-band layer, followed by a continuous metallic ground plane. The presence of this final ground plane improves the overall directivity of the reflectarray.

TABLE I: Geometrical Parameters of the Unit Cell

Parameters	P_X	L_X	h_X	P_L	L_L	h_L
Values (mm)	12	5-8	3.5	96	40-90	9.25

III. Design Approach

Figure 2 illustrates the overall design workflow adopted in this project for the synthesis of the dual-band reflectarray. The process begins with the definition of the reflectarray geometry, including the spatial coordinates of the unit-cell centroids and other design parameters, which serve as the input to the MATLAB-based design framework.

Within MATLAB, a single iterative procedure is employed to determine the reflectarray layout at X-band. For the X-band design, a normally incident plane wave ($\theta^{\text{inc}} = 0°$, $\phi^{\text{inc}} = 0°$) is assumed, allowing the reflection response of the X-band unit cells to be evaluated without explicitly accounting for variations in the angle of incidence. The resulting X-band layout is then passed to CST Microwave Studio for full-wave electromagnetic simulation.

As illustrated in Fig. 3, multiple representative L-band unit cells are shown, each illuminated under a different angle of incidence. For each L-band unit cell, a corresponding X-band layout is taken into account when calculating the reflection coefficient, thereby capturing the effects of both realistic X-band geometries and the true angle of incidence on the L-band response. The angles of incidence at each L-band unit cell is determined from geometrical considerations and used in the unit cell simulation. Since the X-band design is completed at this stage, each true X-band layer is placed into the L-band unit cell simulation to improve accuracy. The extracted reflection response is subsequently returned to MATLAB and used to determine the L-band reflectarray layout.

This bidirectional interaction between MATLAB and CST is carried out within a single loop for the X-band design and within an iterative loop for the L-band design. The final outcome of this bidirectional interaction between MATLAB and CST the workflow is the complete reflectarray layout at both X-band and L-band frequencies, generated within a unified and computationally efficient framework.

The phase response of the X-band unit cell is shown in Fig. 4 at three different X-band frequencies for various angles of incidence. The results demonstrate the robustness of the X-band unit-cell design with respect to variations in the angle of incidence, indicating that incorporating the actual angle of incidence into the X-band design is not necessary. As a result, the computational cost is significantly reduced, particularly since the number of X-band elements in the array is substantially larger than that of the L-band elements.

IV. Results

Figure 5 presents a perspective view of the proposed dual-band reflectarray as implemented in CST Microwave Studio. The antenna integrates X-band metallic elements and an L-band ground plane with patterned slots, which serves as the effective ground plane for the X-band layer, while the slots

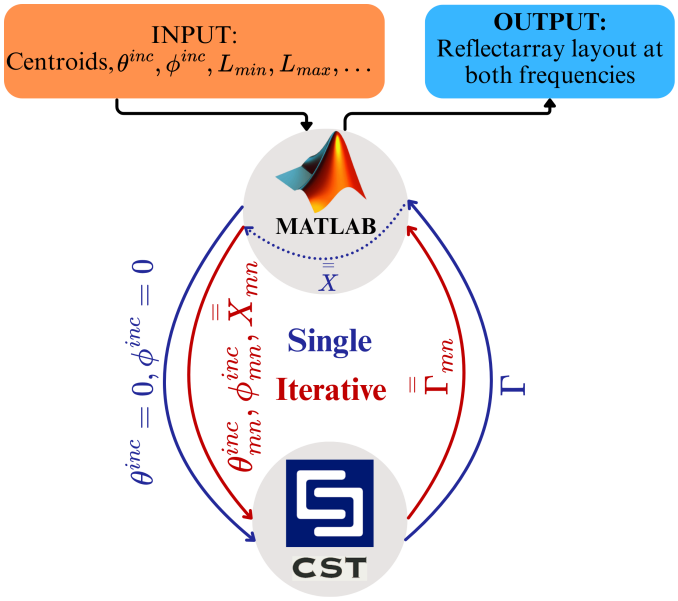

Fig. 2: Matlab-CST interface for calculating the L-band reflection dyad, incorporating the AoI and actual X-band layer.

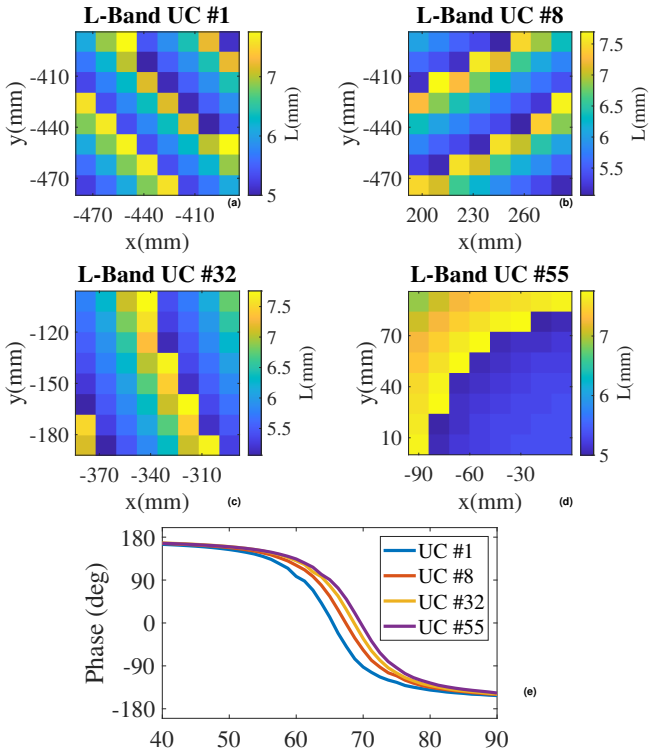

Fig. 3: Actual X-band layout for different L-band unit cells.

introduced in the L-band layer are not electromagnetically visible to the X-band operation. This configuration demonstrates the practical realization of the proposed design approach and confirms the feasibility of accommodating two widely separated frequency bands within a shared aperture without mutual performance degradation.

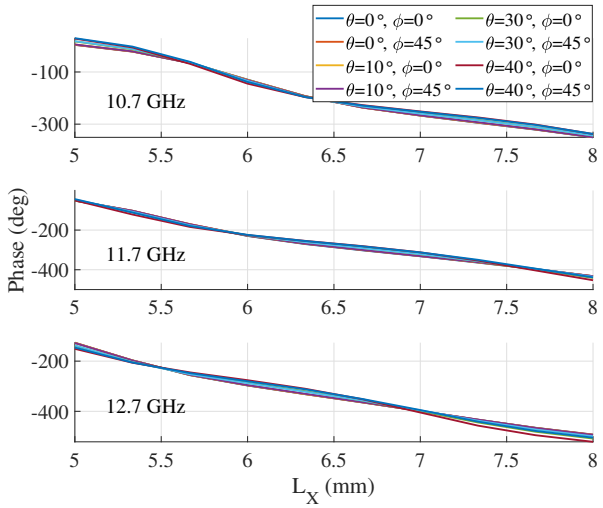

Fig. 4: The phase response of X-band unit cell for different angles of incidence, showing minimal sensitivity to the incidence angle.

The physical aperture of the reflectarray measures $960\ \text{mm} \times 960\ \text{mm}$, corresponding to approximately 5.2λ at the L-band operating frequency of 1.62125 GHz and 37.45λ at the X-band operating frequency of 11.7 GHz. The L-band layer consists of a 10×10 array of unit cells, resulting in a total of 100 cross-shaped slot elements etched in the ground plane. In contrast, the X-band layer employs an 80×80 array of metallic elements, yielding a total of 6400 X-band elements distributed on the top layer.

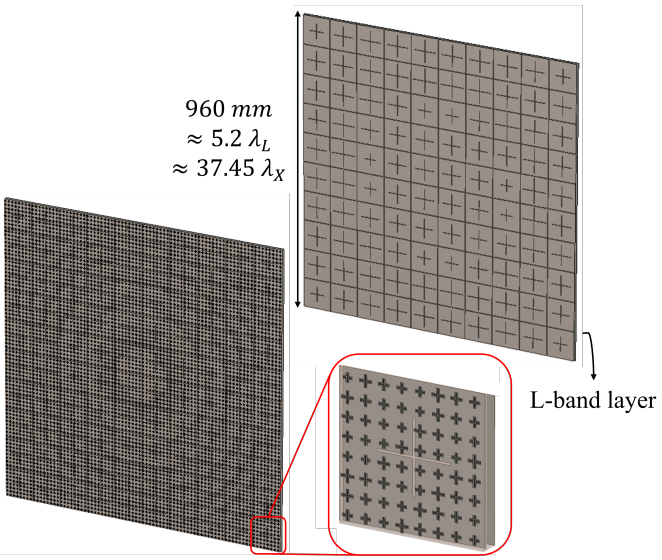

Fig. 5: Perspective view of the dual-band reflectarray, implemented in CST Microwave Studio.

The reflectarray is excited using a cosine-q feed model with horizontal polarization. The feed illumination is characterized by a cosine-q radiation pattern with $q = 3$. The feed is centrally located and positioned at a focal distance of $0.77D$ from the reflectarray aperture, corresponding to an F/D ratio of 0.77, where D denotes the physical aperture width of the reflectarray, equal to 960 mm.

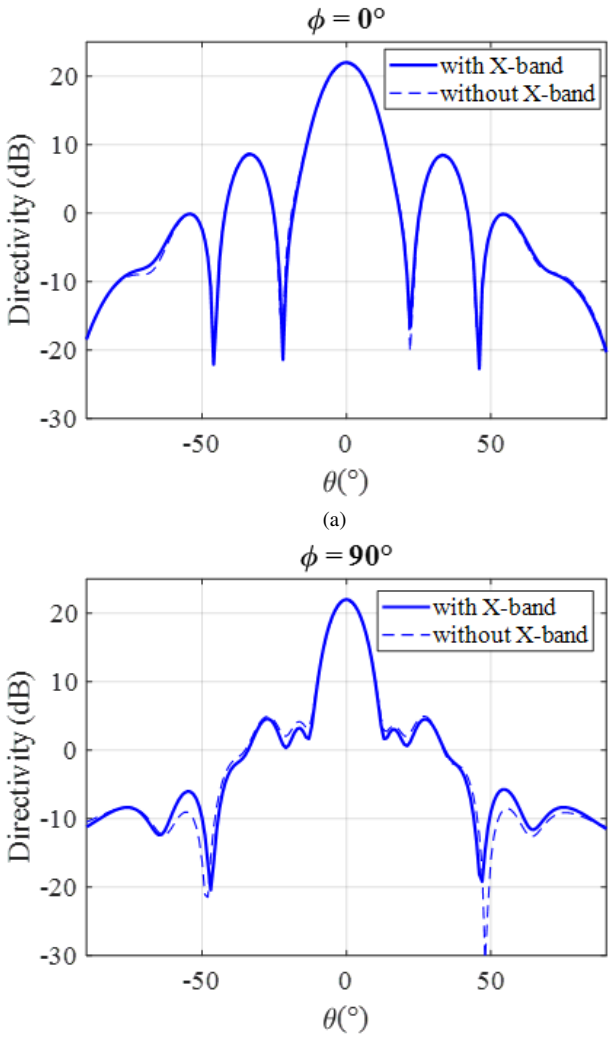

Fig. 6: Farfield radiotion pattern at 1.62125 GHz, (a) E-plane (b) H-plane.

The simulated far-field radiation pattern of the reflectarray at the L-band operating frequency of 1.62125 GHz is shown in Fig. 6. Figures 6(a) and 6(b) illustrate the E-plane and H-plane radiation patterns, respectively. The results demonstrate that the presence of the X-band metallic elements does not perturb the L-band radiation characteristics. This behavior is consistent with the expectation that the X-band structures behave as an approximately uniform impedance sheet at L-band frequencies. Figure 7 shows the simulated far-field radiation pattern at the X-band operating frequency of 11.7 GHz for both the E-plane and H-plane. As observed in Fig. 7(a) and 7(b), the reflectarray produces a directive main beam with a well-defined radiation pattern. The results confirm that the introduction of ground-plane cuts for L-band operation does not degrade the X-band performance in terms of beam formation and radiation behavior.

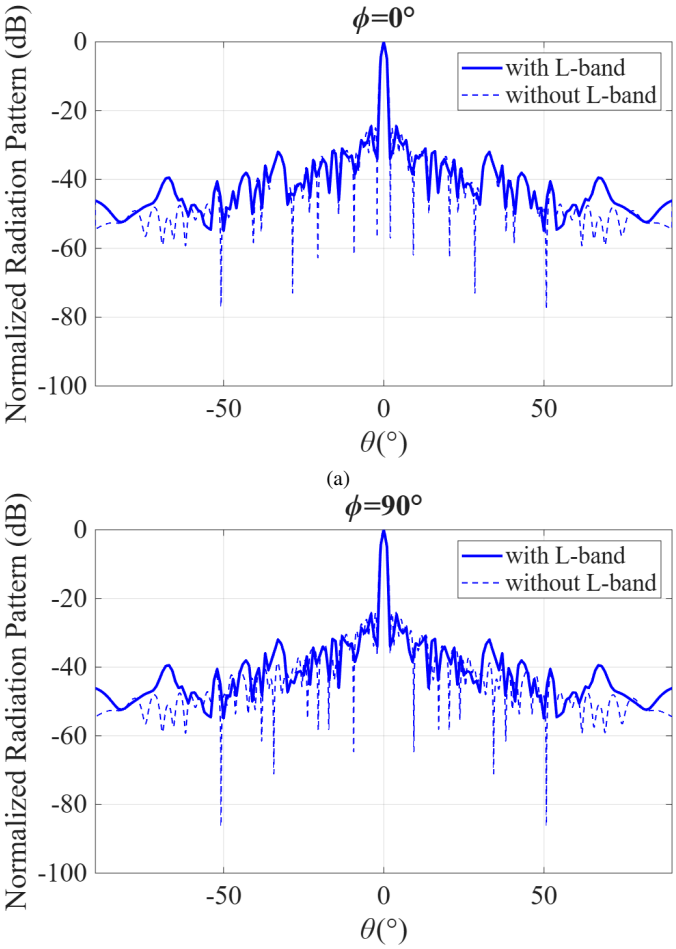

Fig. 7: Farfield radiotion pattern at 11.7 GHz, (a) E-plane (b) H-plane.

V. Discussion and Conclusion

This work demonstrates that the proposed dual-band unit-cell architecture enables independent operation at X-band and L-band despite the significant separation between the two frequency ranges. By employing ground-plane slots as the phase-controlling elements for the L-band, the need for additional metallic structures is eliminated, allowing the X-band elements to operate without degradation. Conversely, the X-band metallic structures exhibit negligible influence on the L-band response, consistent with their behavior as an approximately uniform impedance sheet at lower frequencies.

The simulated radiation patterns at both operating bands confirm that the proposed reflectarray maintains stable beam formation and satisfactory radiation performance at each frequency. These results validate the effectiveness of the proposed design methodology in mitigating mutual coupling and electromagnetic interference between the two bands, while avoiding the blockage and complexity typically associated with multilayer reflectarray configurations.

Overall, the proposed approach provides a practical and efficient solution for realizing widely separated dual-band reflectarrays. This design strategy is particularly well suited for applications requiring dual-frequency operation such as radio astronomy inteference nulling [1]–[4].

Acknowledgement

This work was supported in part by National Science Foundation grant AST-2128506.

References

[1] J. Budhu, S. V. Hum, S. Ellingson, and R. M. Buehrer, "Design of rim-located reconfigurable reflectarrays for interference mitigation in reflector antennas," *IEEE Trans. Antennas Propag.*, vol. 72, no. 4, pp. 3736–3741, Apr. 2024.

[2] F. Sadr, N.-R. Hui, J. Budhu, S. V. Hum, and S. Ellingson, "Applications of reflectarray technology for radio astronomy interference mitigation," in *Proc. 19th Eur. Conf. Antennas Propag. (EuCAP)*, 2025, pp. 1–5.

[3] J. Budhu, S. V. Hum, S. Ellingson, and R. M. Buehrer, "Loading rims of radio telescopes with reconfigurable reflectarrays for adaptive null-steering," in *Proc. USNC-URSI Natl. Radio Sci. Meeting (NRSM)*, 2024, pp. 371–372.

[4] N. J. G. Fonseca, M. Del Mastro, F. Sadr, J. Budhu, G. Mazingue, L. Mangenot, M. Romier, and N. Capet, "Wideband reflectarray design for CubeSat applications in X-band," in *Proc. 19th Eur. Conf. Antennas Propag. (EuCAP)*, 2025, pp. 1–5.